Published online 14 December 2021

Nucleic Acids Research, 2022, Vol. 50, No. 2 ***975–988***
https://doi.org/10.1093/nar/gkab1217

An epigenetic switch activates bacterial quorum sensing and horizontal transfer of an integrative and conjugative element

Joshua P. Ramsay[1,*,†], Tahlia R. Bastholm[1,†], Callum J. Verdonk[2,1], Dinah D. Tambalo[3], John T. Sullivan[4], Liam K. Harold[4], Beatrice A. Panganiban[1], Elena Colombi[1], Benjamin J. Perry[4], William Jowsey[4], Calum Morris[4], Michael F. Hynes[5], Charles S. Bond[2], Andrew D.S. Cameron[3], Christopher K. Yost[3] and Clive W. Ronson[4,*]

[1]Curtin Medical School and Curtin Health Innovation Research Institute, Curtin University, Perth, WA 6102, Australia, [2]School of Molecular Sciences, University of Western Australia, Perth, WA 6009, Australia, [3]Biology Department, University of Regina, Regina, SK S4S 0A2, Canada, [4]Department of Microbiology and Immunology, University of Otago, Dunedin, 9016, New Zealand and [5]Department of Biological Sciences, University of Calgary, Calgary, AB T2N 4V8, Canada

Received July 22, 2021; Revised November 23, 2021; Editorial Decision November 24, 2021; Accepted November 25, 2021

ABSTRACT

Horizontal transfer of the integrative and conjugative element ICE*Ml*Sym^{R7A} converts non-symbiotic *Mesorhizobium* spp. into nitrogen-fixing legume symbionts. Here, we discover subpopulations of *Mesorhizobium japonicum* R7A become epigenetically primed for quorum-sensing (QS) and QS-activated horizontal transfer. Isolated populations in this state termed R7A* maintained these phenotypes in laboratory culture but did not transfer the R7A* state to recipients of ICE*Ml*Sym^{R7A} following conjugation. We previously demonstrated ICE*Ml*Sym^{R7A} transfer and QS are repressed by the antiactivator QseM in R7A populations and that the adjacently-coded DNA-binding protein QseC represses *qseM* transcription. Here RNA-sequencing revealed *qseM* expression was repressed in R7A* cells and that RNA antisense to *qseC* was abundant in R7A but not R7A*. Deletion of the antisense-*qseC* promoter converted cells into an R7A*-like state. An adjacently coded QseC2 protein bound two operator sites and repressed antisense-*qseC* transcription. Plasmid overexpression of QseC2 stimulated the R7A* state, which persisted following curing of this plasmid. The epigenetic maintenance of the R7A* state required ICE*Ml*Sym^{R7A}-encoded copies of both *qseC* and *qseC2*. Therefore, QseC and QseC2, together with their DNA-binding sites and overlapping promoters, form a stable epigenetic switch that establishes binary control over *qseM* transcription and primes a subpopulation of R7A cells for QS and horizontal transfer.

INTRODUCTION

Mobile genetic elements (MGE) contribute to prokaryotic evolution by moving DNA within and between genomes. Gene acquisition events facilitated by MGE are pivotal to the diversification and competitive success of bacteria (1). Conjugative plasmids and integrative-and-conjugative elements (ICEs) disseminate large clusters of genes that endow competitive advantages upon their hosts in particular niches (2). Horizontal transfer can benefit both the recipient bacterium and the MGE, but horizontal transfer may also impart fitness costs on donor cells (1,3,4). The negative impacts of MGE transfer on the bacterial host have likely favored the evolution of MGE that activate transfer infrequently in response to multiple endogenous and environmental cues. This may involve mechanisms that ensure only a small proportion of the cell population act as donors (5–8). In this work, we describe how the *Mesorhizobium japonicum* R7A (formerly *M. loti* R7A (9)) symbiosis island ICE*Ml*Sym^{R7A} controls a differentiation event that produces a sub-population of cells that transfer ICE*Ml*Sym^{R7A} at higher frequency. This state termed R7A* is vertically inherited but resets in recipients following horizontal transfer of ICE*Ml*Sym^{R7A}.

Mesorhizobia are soil bacteria that can host ICEs known as ICESyms carrying genetic cargo essential for establish-

*To whom correspondence should be addressed. Tel: +61 8 9266 1152; Email: Josh.Ramsay@curtin.edu.au
Correspondence may also be addressed to Clive W. Ronson. Email: Clive.Ronson@otago.ac.nz
†The authors wish it to be known that, in their opinion, the first two authors should be regarded as Joint First Authors.

ment of a nitrogen-fixing symbiosis with legumes (10–12). Following transfer to non-symbiotic *Mesorhizobium* recipients, ICESyms integrate into *Mesorhizobium* spp. chromosomes by recombining with the 3′ ends of highly conserved chromosomal genes and the recipients gain the ability to induce nitrogen-fixing root nodules on specific legume hosts. For example, ICEs in *Mesorhizobium* spp. have been identified that specify symbioses with species of *Lotus*, *Biserrula* and *Cicer* (12–14). ICESyms carry a complement of conserved core genes required for their excision and conjugation (12,15–18) and orthologs of these genes are identifiable on ICEs and plasmids throughout the proteobacteria (15), suggesting this large family of conjugative elements has evolved from a highly successful common ancestor. The paradigm ICESym, ICE*Ml*Sym^{R7A}, was identified in *M. japonicum* R7A following *in situ* transfer of the ICE to indigenous non-symbiotic mesorhizobia in New Zealand soils, where transfer converted recipients into symbionts of the pasture legume *Lotus corniculatus* (14,19). ICE*Ml*Sym^{R7A} integrates into the 3′ end of the sole *phe*-tRNA gene in R7A and other mesorhizobia through site-specific recombination facilitated by the recombinase/integrase IntS (14).

ICE*Ml*Sym^{R7A} excision from the chromosome and subsequent conjugative transfer is activated by small diffusible *N*-acyl-homoserine lactones (AHL), a phenomenon known as quorum sensing (QS) (Figure 1). The LuxR-family QS protein TraR encoded by ICE*Ml*Sym^{R7A} activates transcription of the *traI1* gene also present on ICE*Ml*Sym^{R7A}. The AHL synthase TraI1 then produces *N*-(3-oxohexanoyl)-L-homoserine lactone (3-oxo-C6-HSL) as the major AHL product (16). As well as activating *traI1* and AHL production, TraR stimulates ICE*Ml*Sym^{R7A} excision and conjugative transfer by activating transcription of the transcriptional activator FseA encoded in a separate operon downstream of the *traR* gene. The FseA sequence is coded across two open-reading frames *msi172* and *msi171*. A low-frequency programmed + 1 ribosomal frameshift occurs within the 3′ end of *msi172* fusing the coding sequences of *msi172-msi171* culminating in production of a single polypeptide. FseA activates transcription of the *rdfS* promoter, which stimulates expression of the recombination directionality factor RdfS, the prepilin peptidase TraF and the lytic transglycosylase Msi107 and leads to ICE*Ml*Sym^{R7A} excision and transfer (16,18) (Figure 1A).

In wild-type R7A populations, the activation cascade stimulating ICE*Ml*Sym^{R7A} excision and transfer is strongly repressed. Production of 3-oxo-C6-HSL is barely detectable in stationary-phase cultures and ICE*Ml*Sym^{R7A} is excised in only ∼5% of cells. Such cultures transfer ICE*Ml*Sym^{R7A} at a rate of 10^{-6} to 10^{-5} per donor cell. In the majority of R7A cells in the population, TraR and FseA are both independently inhibited through protein–protein interactions with the antiactivator QseM (15,18) (Figure 1). A *qseM* deletion mutant R7AΔ*qseM* exhibits close to 100% ICE*Ml*Sym^{R7A} excision in stationary-phase cells, 1000-fold increased conjugative transfer and increased AHL production. Importantly, ICE*Ml*Sym^{R7A} excision in R7AΔ*qseM* does not result in loss of ICE*Ml*Sym^{R7A}. While our culture medium does not provide any known selection for maintenance of ICE*Ml*Sym^{R7A}, we have never observed spontaneous loss of ICE*Ml*Sym^{R7A} from R7A or R7AΔ*qseM* cells during laboratory culture. Like several other ICEs (21), ICE*Ml*Sym^{R7A} likely maintains itself in the excised state through rolling-circle replication initiated by its conjugative relaxase, as relaxase mutants do not maintain the excised ICE (16). Furthermore, ICE*Ml*Sym^{R7A} excision in R7AΔ*qseM* remains growth-phase and QS-dependent, as ICE*Ml*Sym^{R7A} reintegrates into the chromosome in most cells during exponential growth when AHL concentrations are low and therefore *rdfS* is not expressed. In this sense, R7AΔ*qseM* cells are primed for transfer, but excision and transfer remain conditional on QS activation. Overexpression of *qseM* represses excision of ICE*Ml*Sym^{R7A} to levels below that observed in wild-type R7A populations, indicating that *qseM* expression is repressed in the ∼5% of cells in wild-type populations carrying the excised form of ICE*Ml*Sym^{R7A} and suggesting that these cells are likely primed for ICE*Ml*Sym^{R7A} transfer like R7AΔ*qseM*. R7A populations are therefore likely a mixture of transfer-repressed (QseM expressed) and transfer/QS-enabled (*qseM* repressed) cells (Figure 1B).

Transcription of *qseM* is regulated by a helix-turn-helix protein QseC, encoded by the divergently transcribed *qseC* gene (Figure 1) (15). QseC dimers bind each of two operator sequences O_L and O_R that overlap divergent promoters for *qseM* and *qseC*. QseC preferentially binds O_L and appears to only strongly bind O_R in the presence of QseC-bound O_L, indicating cooperativity. The P*qseC* promoter -35 region is positioned within O_R and QseC activates P*qseC* transcription (15). The -35 region of the P*qseM* promoter is also positioned within the O_R site on the opposite DNA strand. Deletion of *qseC* leads to increased expression of QseM, which in turn inhibits ICE*Ml*Sym^{R7A} excision and conjugative transfer and prevents TraR-mediated activation of AHL production (15). We have postulated that QseM, QseC, O_L and O_R together with the overlapping *qseC* and *qseM* promoters comprise a molecular switch that derepresses QS and ICE excision in the ∼5% of cells carrying an excised copy of ICE*Ml*Sym^{R7A} in stationary-phase populations of R7A (15).

QseC and its operator sequences share striking similarities with the controller (C) proteins and DNA operator sites of several type II restriction–modification (RM) systems (15,22). C proteins are dimeric proteins that together with their adjacent DNA operators and overlapping promoters form molecular switches that orchestrate the delay between DNA methyltransferase gene expression and subsequent restriction endonuclease gene expression following entry of an RM module into a naïve cell (22–25). Once RM systems are established in the cell, C proteins stably maintain appropriate levels of endonuclease and methyltransferase expression throughout DNA replication and cell division. This stability is achieved through complex positive and negative autoregulatory mechanisms that, like the *qseC-qseM* locus, often involve two adjacent operator sites controlling divergent overlapping promoters. While QseC itself is not associated with RM systems, it was one of the proteins found in a systematic search for C proteins in microbial genomes and was classified as C.PvuII family (motif 4)-like (22). Like C.PvuII, QseC binds dual operator sites between two overlapping divergent promoters, shows strong

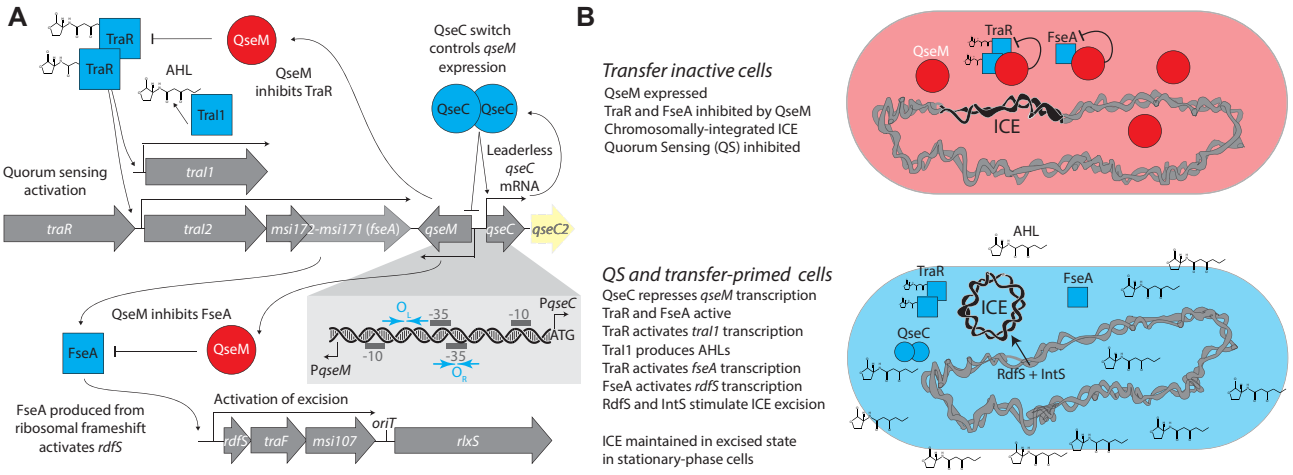

Figure 1. Model of excision and transfer regulation by genes encoded on ICE*Ml*Sym^{R7A}. (**A**) Gene maps of the *traR-qseC2* and *rdfS-rlxS* regions present on ICE*Ml*Sym^{R7A} are shown with a schematic detailing the molecular activation and repression of QS and ICE*Ml*Sym^{R7A} excision and transfer. Proteins with a positive effect on QS, excision and conjugative transfer are shown in blue, while the QseM antiactivator is shown in red. In cells active for QS, AHLs produced by TraI1 activate TraR which activates transcription from two *tra* boxes, located upstream of *traI1* and the likely pseudogene *traI2* (16). *traI2* forms an operon with two open-reading frames *msi172* and *msi171*. A single polypeptide product, FseA, is translated from *msi172-msi171* following a programmed + 1 ribosomal frameshift encoded within the 3′ end of *msi172* (18). FseA activates transcription from the *rdfS* promoter and RdfS stimulates ICE*Ml*Sym^{R7A} excision and transfer (17,20). *rdfS* is coded upstream of genes encoding the conjugative prepilin peptidase TraF, the lytic transglycosylase Msi107 and the conjugative relaxase RlxS. In cells repressed for QS, the antiactivator QseM binds TraR and FseA, inhibiting their ability to act as transcriptional activators. The QseC protein controls expression of QseM. QseC both activates its own gene promoter from a leaderless mRNA and represses *qseM* expression. A schematic illustrating the overlapping -35 regions of the *qseC* and *qseM* promoters (P*qseC* and P*qseM*) and the QseC binding regions O_L and O_R is shown in the shaded box. Note the role of *qseC2* (shown in yellow) is not incorporated in this model yet as it had not been studied prior to this work. (**B**) Illustration and summary of the features of cells that are either in a transfer-repressed state expressing QseM (shaded red) or those repressed for *qseM* expression (in blue), which participate in QS and maintain an excised ICE in stationary-phase populations and exhibit elevated rates of conjugation.

preference for the left operator sequence (O_L) and binds co-operatively with QseC-O_L to the right operator sequence O_R. Also like several C proteins, QseC is translated from a leaderless mRNA (15,26,27). At least six distinct families of QseC/C-protein-like genes are present adjacent to *qseM* homologues on ICEs identified throughout the alphaproteobacteria. In addition, genes for several members of the same C-protein families are positioned adjacent to the QS antiactivator gene *traM* on QS-regulated *Agrobacterium* and *Rhizobium* spp. plasmids, indicating they may also regulate QS and transfer induction for these plasmids (15,28).

On ICE*Ml*Sym^{R7A} a second C-protein gene, *qseC2*, is located directly downstream of *qseC* (Figure 1). QseC2 resembles the C.EcoRV family (motif 7 (22)) of C proteins. C.EcoRV, like C.PvuII and QseC, binds dual operator sites between divergent overlapping promoters (29,30). Two adjacent putative operator sequences (hereafter, $O2_L$ and $O2_R$) each containing the sequence ATCC-N_7-GGAT are positioned between the 3' end of *qseC* and the 5' end of *qseC2* (15). There are several other examples of tandemly coded C-protein genes like *qseC* and *qseC2* on ICEs (15,31). Previously, we speculated that they may represent remnants of C-protein gene replacements and indeed, several appear to be pseudogenes (15,32); however, others have suggested tandem C-protein genes may comprise higher-order regulatory switches (22).

It is not clear how the balance between molecular components in the ICE*Ml*Sym^{R7A} QS and transfer regulon is tipped to promote entry into a transfer-primed state through repression of *qseM*. Furthermore, it is unclear if this switch is transient or persistent through cell division once established. In this work, we report that approximately 2% of colonies formed by wild-type R7A contain isolatable cells that have entered a *qseM*-repressed state we herein name R7A*. R7A* cells are derepressed for QS, ICE excision and conjugative transfer, similar to the phenotypes observed for R7AΔ*qseM*. Isolated R7A* cells vertically inherited their QS and transfer-primed state under standard culture conditions. Extensive genome sequencing did not identify any mutations likely to explain these phenotypes. Using RNA-seq and a variety of genetic and molecular manipulations, we demonstrate that QseC2-mediated repression of antisense-*qseC* transcription is the first step required for R7A* differentiation, which, once established, is maintained by QseC2 and QseC acting in concert.

MATERIALS AND METHODS

Microbiological techniques

Bacteria were cultured as described previously (16,17,33,34) and further detail is available in the Supporting Information. Strains and plasmids are listed in Supplementary Table S1. Oligonucleotides used in construction of plasmids are listed in Supplementary Table S2. Growth curves, DNA extraction, plasmid construction, mutagenesis, QPCR, CV026 bioassays, β-galactosidase assays and bacterial conjugation assays (Supplementary Table S3) were carried out as previously described (15,18,35).

Competition assays

Plasmids pFAJ1700 and pFAJ1700:neo were introduced into both R7A and R7A* individually. R7A(pFAJ1700) and R7A*(pFAJ1700:neo) were adjusted for density and combined in equal ratio. The same experiment was also carried out with R7A(pFAJ1700:neo) and R7A*(pFAJ1700). Colony-forming units for each strain were calculated after 24, 48 and 72 h. The entire experiment was repeated three times. Further details are provided in Supporting Information and Supplementary Figure S1.

Phenotypic microarrays

TY cultures of R7A, R7A* and R7AΔ*qseM* were grown at 28°C with shaking to stationary phase and diluted to an OD_{600} of 0.05. Cells were washed sequentially in liquid RDM lacking a carbon source four times in 1 ml, 700 μl, 500 μl and 200 μl volumes. Cells were then resuspended in liquid RDM containing Redox Dye Mix MA (Biolog). One hundred microlitres of cell suspension were added to each well of PM1 and PM2A 96-well 'carbon sources' microplates (Biolog) and the plates were then incubated in the dark at 28°C with shaking for 72 h. For the PM1 plates measurements of redox dye absorbance at 540 nm and OD_{600} were taken every eight hours throughout growth on an EnSight Multimode Plate Reader (Perkin Elmer). Example OD_{600} measurements for each strain grown in PM1 plates are presented in Supplementary Figure S2. Measurements for PM2A plates were taken only at the 72 h time point (data not shown). Experiments were repeated twice for each strain. No consistent differences were observed for carbon-source utilisation between any of the strains on either the PM1 or PM2A plates.

Genome sequencing and assembly

Expanded methods for genome sequencing, assembly and whole-genome comparisons can be found in Supporting Information. Briefly, DNA for use in Oxford Nanopore Technologies MinION sequencing (R.9.4.1 flowcells and MinION Mk1B) was extracted to maximize read length as described in Supporting Information. Approximately 2.7 and 5.7 gigabases of sequence was generated for R7A and R7A* respectively. Reads were filtered by quality (>q10) and size (>8 kb), producing ∼190-fold read depth for initial assemblies using Flye (36). Assemblies were polished five times with filtered nanopore reads using Racon (https://github.com/isovic/racon), four times using Medaka (https://github.com/nanoporetech/medaka) and five times using Pilon (37) with Illumina sequencing reads (560- and 252-fold read depth for R7A and R7A*, respectively). Both short and long reads were aligned to penultimate assemblies and compared (Dataset S1) with the previous R7A assembly (Genbank accession CP033366.1). Mapped reads and potential variants were manually inspected and assessed as described in Supporting Information and Dataset S1. One nucleotide variant was ambiguous in both Nanopore and Illumina reads and was further assessed using PCR and Sanger sequencing in both R7A and R7A*, which revealed no difference in sequence. Genbank accessions for the final reference sequences for *M. japonicum* R7A and R7A* are CP051772.1 and CP051773.1, respectively.

Transcriptome sequencing

Detailed description of RNA sequencing methods and differential expression analyses can be found in Supporting Information. Briefly, RNA was extracted from duplicate early-stationary-phase TY cultures (48 h) for R7A and R7A* (see Supplementary Figure S1A for example growth curves). Libraries were sequenced on an Illumina MiSeq using 75-bp paired-end sequencing as described further in Supporting Information. Reads were mapped to the R7A genome (CP051772.1). A summary of differentially regulated ICE*Ml*Sym^{R7A} regulatory genes is presented in Supplementary Table S4 and genome-wide transcriptome data and statistics can be found in Dataset S2.

DNA-binding assays

Protein purification of 6H-QseC and 6H-QseC2 was carried out as described previously for 6H-QseC (15), with adjustments described in Supporting Information. EMSAs were carried out as previously described (38). DNA containing the $O2_L$ and $O2_R$ operators and scrambled derivatives were synthesized and amplified by PCR using IRDye800-labeled DNA oligonucleotides as primers (Supplementary Table S2). The *qseC2* operator sites were amplified by PCR from synthesized DNA and then labeled in a second PCR using IRDye800-labeled primers (Supplementary Table S2). Binding reactions were conducted in a similar manner to those carried out previously (38) and detailed EMSA methods are provided in Supporting Information. Reusable DNA Capture Technology (ReDCaT) approach was used for SPR DNA-binding experiments (39) using the Biacore T200 (GE Healthcare) and Biacore SA sensor chip (GE Healthcare). Oligonucleotides used in generation of the ReDCaT chip and ReDCaT assays are listed in Supplementary Table S2. SPR assays were carried out as previously described (38) and as further detailed in Supporting Information and Supplementary Table S5.

RESULTS

Quorum-sensing high-frequency ICE*Ml*Sym^{R7A} donors arise spontaneously in R7A populations

Following passaging of *M. japonicum* R7A colonies on solid defined medium (Glucose (G)/RDM), a phenotypic variant of R7A was serendipitously isolated, termed R7A*. Unlike wild-type R7A, R7A* induced violacein production in the AHL biosensor strain *Chromobacterium violaceum* CV026 (Figure 2A). The transfer frequency of ICE*Ml*Sym^{R7A} from R7A* to the recipient R7ANS, a derivative of R7A cured of ICE*Ml*Sym^{R7A} (17), was approximately 400-fold greater than that observed when wild-type R7A was used as donor (Supplementary Table S3), but around 2–3-fold less than when R7AΔ*qseM* was used. Excised ICE*Ml*Sym^{R7A} was detected in 3–4% of log-phase R7A* populations and 75–87% of those stationary-phase R7A* populations using an established quantitative PCR assay (17). In comparison, ICE*Ml*Sym^{R7A} excision in R7A

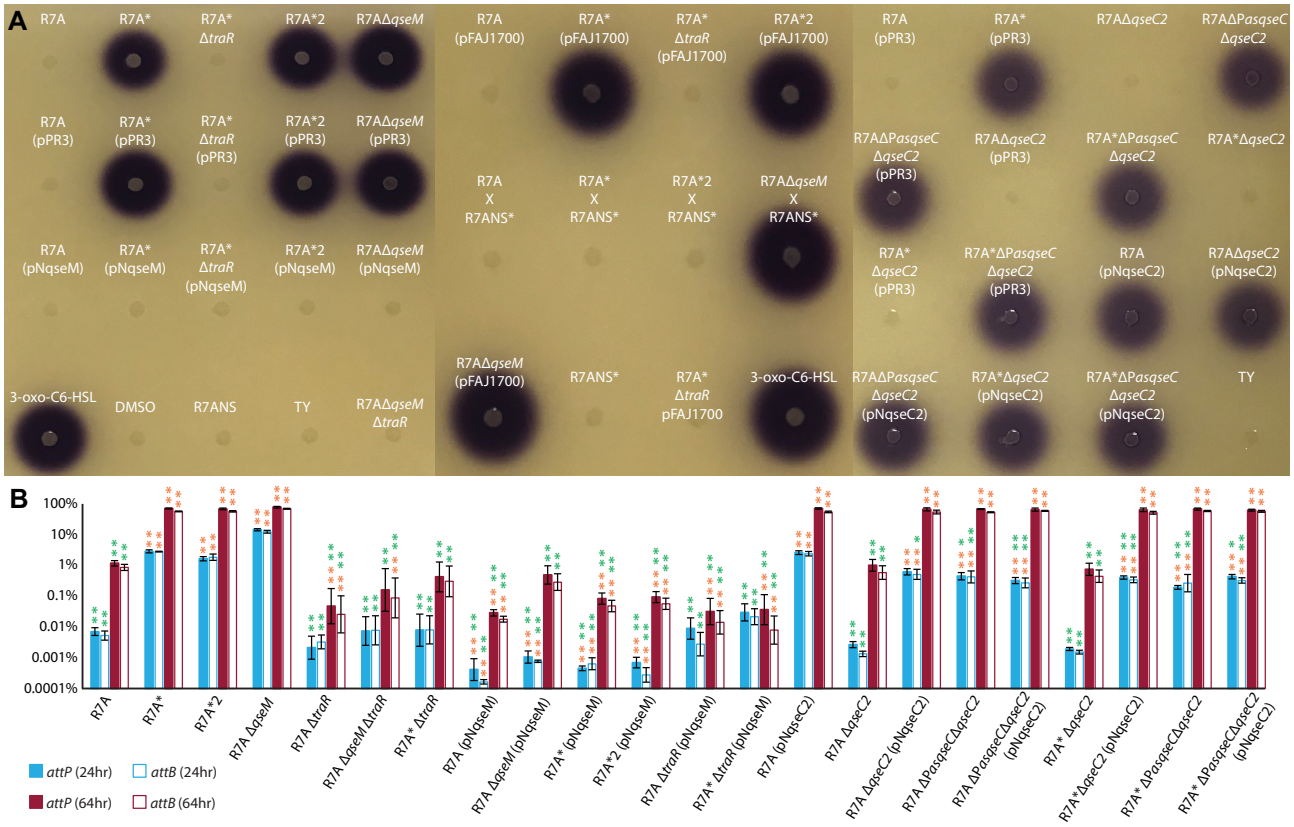

Figure 2. Quorum sensing and ICE*Ml*Sym^{R7A} excision phenotypes of R7A* and derivatives. (**A**) *Chromobacterium violaceum* CV026 bioassays were used to detect AHLs in broth-culture supernatants. Three 25-cm plates are shown. Supernatants from R7A* exconjugants in which ICE*Ml*Sym^{R7A} was reintroduced into the R7ANS* background are labeled as 'Donor X R7ANS*'. Vector-only (pPR3 and pFAJ1700), positive (10 μM 3-oxo-C6-HSL) and negative controls (DMSO, R7ANS, TY) are included for comparison. (**B**) Quantitative PCR assays of ICE*Ml*Sym^{R7A} excision. Strains were grown in liquid TY medium and sampled in log phase (24 h) and late stationary phase (64 h). DNA was extracted and assayed by quantitative PCR. PCR primers amplify products that span the circular ICE*Ml*Sym^{R7A} DNA (*attP*) and vacant chromosomal insertion sites (*attB*) and these are presented as the percentage of total chromosomes in the sample, measured by amplification of the chromosomal *melR* gene (17). Bars indicate the average percentage and standard deviation (error bars) of three replicate experiments. The *y*-axis is in log-scale. A one-way ANOVA followed by Tukey's post-hoc test was carried out for comparisons between R7A and every other strain and for comparisons between R7A* and every other strain. Green asterisks indicate the mean is statistically different from R7A* at the same time point (* 0.05, ** $P < 0.01$) and orange asterisks indicate the mean is statistically different from R7A at the same time point (* $P < 0.05$, ** $P < 0.01$). Vector-only controls are presented in Supplementary Figure S3.

was <0.01% at log phase and 1–2% at stationary phase, while ICE*Ml*Sym^{R7A} excision in R7AΔ*qseM* was ∼20% in log-phase and ∼100% stationary-phase (Figure 2B). Therefore R7A* cells appear to exist in a state similar to that seen for R7AΔ*qseM* except that they exhibit slightly lower frequencies of ICE*Ml*Sym^{R7A} excision and conjugative transfer.

To determine how frequently R7A cells differentiated into R7A*, 500 single colonies isolated from plating a stationary-phase liquid R7A culture on G/RDM were tested for the ability to induce violacein production when streaked adjacent to CV026 (Supplementary Figure S4). Ten individual colonies induced violacein production to varying levels. These colonies were subcultured and single colonies were again tested for AHL production, which revealed they contained mixtures of R7A and R7A*-like cells. Further single-colony purification led to isolation of stable R7A*-like cell lines which induced CV026 in a similar manner to the original R7A* (Figure 2A). Examination of one of these isolates, named R7A*2, revealed it exhibited near-identical excision and transfer frequencies to R7A* (Figure 2B and Supplementary Table S3). The R7A* isolation experiment was repeated twice more and, in each case, ∼2% of single colonies contained mixed subpopulations of cells exhibiting R7A and R7A*-like phenotypes. The consistent appearance of R7A* cells within 2% of single colonies that contained subpopulations of both R7A and R7A*-like cells suggested that the R7A* phenotype was arising stochastically within these colonies following plating.

R7A* cells do not exhibit reduced fitness or readily revert to R7A under laboratory conditions

Despite the differences in ICE*Ml*Sym^{R7A} excision, no differences in growth rate were observed between R7A, R7A* or R7AΔ*qseM* cells in either complex or defined medium. Moreover, examinations of mixed liquid cultures of R7A and R7A* did not reveal any competitive differences in growth (Supplementary Figure S1). Phenotypic microarrays also failed to reveal any differences in carbon-source utilization (see Materials and Methods and Supplementary Figure S2). In previous work, we found overexpression of

rdfS is lethal for R7A aside from a small proportion of cells that survive through curing of ICE*Ml*Sym^{R7A} (17); similarly, overexpression of *msi172-msi171* (*fseA*) (16), which activates *rdfS* expression, results in lethality. Interestingly, attempts to introduce pJRtraR (expressing *traR* downstream of its native promoter) into R7A* and R7AΔ*qseM* resulted in the formation of small colonies that ceased growth after 5 days. Since introduction of pJRtraR into wild-type R7A induces AHL production, conjugation and ICE*Ml*Sym^{R7A} excision (16,17), this result suggested that R7A* and R7AΔ*qseM* were sensitive to further QS induction through increased expression of *traR*. Deletion of *msi172*, which abolishes FseA production, in R7A* restored the ability to introduce pJRtraR, indicating that the growth-inhibitory effects of pJRtraR in R7A* were mediated by FseA. In summary, growth inhibition effects were not manifested in R7A* or R7AΔ*qseM* under the conditions tested; however, *fseA*-dependent growth inhibition was induced in R7A* and R7AΔ*qseM* cells as a result of additional *traR* expression from pJRtraR.

Throughout this work we did not observe any reversion of R7A* back to R7A under standard laboratory conditions. We attempted to identify spontaneous revertants of R7A* and R7A*2 using a CV026 screening method similar to that used in the isolation of R7A*2, where we screened 500 colonies for loss of AHL production. While single colonies that exhibited both reduced AHL production and conjugative transfer rates were identified (Supplementary Figure S5 and Table S3), all returned to an R7A* state following passaging, suggesting factors indirectly related to activation of QS predisposed these derivatives to re-establish R7A* phenotypes (see Supporting Information for further details).

The R7A* phenotype is unlikely to be caused by mutation and is reset in recipients of ICE*Ml*Sym^{R7A}

It seemed possible that structural rearrangements or mutations in the R7A* genome might be responsible for the R7A* phenotype. Reference-quality genome sequences were assembled using both long and short-read sequencing of R7A and R7A* DNA (Genbank accessions CP051772 and CP051773). Both assemblies produced 6530403-bp genomes and whole-genome alignments did not reveal any structural differences. The R7A and R7A* sequences differed by three single-nucleotide substitutions in chromosomal regions with no obvious link to transfer or QS. No differences were observed between the ICE*Ml*Sym^{R7A} sequences. R7A*2 DNA was sequenced (CP052769.1) using short-read sequencing and when aligned to the R7A sequence, two synonymous coding-sequence changes were identified, along with a 7-bp deletion in one of five direct repeats in an intergenic region. All three variations in R7A*2 were at distinct loci from those observed in R7A* and again no differences were present within ICE*Ml*Sym^{R7A} (see Supporting Information and Dataset S1 for detailed descriptions of genome assemblies and variant calling).

We next investigated if the R7A* state was maintained following conjugative transfer of ICE*Ml*Sym^{R7A}. Eight exconjugants derived from each of three matings using R7A, R7A* or R7AΔ*qseM* as donors were screened for AHL production. None of the exconjugants receiving ICE*Ml*Sym^{R7A} from R7A or R7A* induced CV026, whereas exconjugants receiving ICE*Ml*Sym^{R7A} from R7AΔ*qseM* induced CV026 as expected (Supplementary Figure S6). Therefore, the R7A* state was not transferred with ICE*Ml*Sym^{R7A} to R7ANS. It seemed possible that the chromosomal background of the R7ANS recipients might somehow suppress the R7A* phenotype following transfer. To discount this possibility, ICE*Ml*Sym^{R7A} was cured from R7A* using plasmid pJR204 that overexpresses RdfS, as described previously (17). The resulting strain R7ANS* was sequenced (CP052770.1) and alignment with the R7A* sequence confirmed loss of ICE*Ml*Sym^{R7A} and identified a single synonymous nucleotide change compared to R7A* (again, this nucleotide change was distinct from others identified, Supporting Information and Dataset S1). R7ANS* was then used as a recipient in conjugation experiments using R7A, R7A* and R7AΔ*qseM* as donors. Conjugation frequencies for all matings were near-identical to those carried out using R7ANS as the recipient (Supplementary Table S3). Eight R7ANS*-derived exconjugants for each mating were examined for AHL production using CV026. Again, none of the exconjugants receiving ICE*Ml*Sym^{R7A} from R7A or R7A* induced CV026 while all those receiving ICE*Ml*Sym^{R7A} from R7AΔ*qseM* did (Supplementary Figure S6). Therefore, the R7A* phenotypes were not transferred with ICE*Ml*Sym^{R7A}, even when ICE*Ml*Sym^{R7A} was transferred into the isogenic R7ANS* chromosomal background obtained by curing ICE*Ml*Sym^{R7A} from R7A*. In summary, these experiments indicate an epigenetic factor was responsible for the R7A* phenotype.

Transcription of the antiactivator gene *qseM* is repressed in R7A*

Given the similarities between R7A* cells and R7AΔ*qseM*, we suspected that *qseM* expression might not be expressed in R7A* cells. pNqseM, which constitutively expresses *qseM* from the *nptII* promoter, was introduced into R7A* and R7A*2. pNqseM abolished AHL production (Figure 2A) and reduced excision to levels below that of R7A (Figure 2B and Supplementary Figure S4). Deletion of *traR* in R7A* and R7AΔ*qseM* had a similar effect (Figure 2), consistent with QS being essential for full activation of ICE*Ml*Sym^{R7A} excision in stationary-phase cells. Interestingly, while R7A*Δ*traR* exhibited a reduced transfer frequency (Supplementary Table S3), it remained around 10-fold higher than that of R7AΔ*traR* for which transfer was barely perceptible. This suggested that even without *traR*, R7A* cells remain partially upregulated for transfer. This is consistent with *qseM* expression being repressed in R7A* and R7A*Δ*traR*, since QseM also independently binds and inhibits FseA (Figure 1A) (18).

RNA-seq experiments were carried out to compare RNA transcript abundance in R7A and R7A*. Abundance of *traI1, traI2, rdfS-msi107* and RNA encoding conjugation pore proteins was increased in R7A* (Supplementary Table S4 and Dataset S2), consistent with the increased rate of excision and conjugative transfer observed (Figure 2B and Supplementary Table S3). Transcripts mapping to *qseM*

were vastly reduced in R7A* compared to R7A (Figure 3). Notably, some of the other pronounced differences observed were in sequencing reads that mapped in the antisense direction to the *msi172-msi171* (*fseA*) and *qseC* regions. The positive-sense *msi172-msi171* (*fseA*) transcript initiating from the *traI2* promoter was marginally increased in R7A*; however, antisense *msi172-msi171* transcripts extending from the *qseM* promoter were 11-fold reduced in R7A* compared to R7A. Similarly, strong antisense transcription of *qseC* observed in R7A was almost completely absent from R7A* (Figure 3 and Supplementary Table S4). Antisense-*qseC* transcription initiated from a previously unrecognized promoter region herein named P*asqseC*, which was positioned downstream of *qseC* and upstream of the putative *qseC2*-associated operator sites $O2_L$ and $O2_R$ (Figure 4A). Both *qseC2* and *qseC* transcripts were present at higher levels in R7A* but only the 1.7-fold increase for *qseC2* R7A* was statistically significant (Figure 3 and Supplementary Table S4).

QseC2 and P*asqseC* control entry into the R7A* state

The differences observed between R7A and R7A* in the RNA-seq data for the P*asqseC-qseC2* region suggested these genes and transcripts had a role in the R7A* phenotypes. To investigate the role of *qseC2*, *qseC2* deletions were constructed in both R7A and R7A* (Figure 4A). In the R7A* background *qseC2* deletion abolished AHL production (Figure 2A) and reduced ICE*Ml*Sym^{R7A} excision (Figure 2B) and conjugative transfer frequencies (Supplementary Table S3) to levels equivalent to those observed for R7A. Introduction of plasmid pNqseC2, expressing *qseC2* from the strong constitutive *nptII* promoter, activated AHL production, excision and transfer in both R7A and R7AΔ*qseC2* strains to levels phenotypically indistinguishable from R7A* (Figure 2, Supplementary Figure S3 and Table S3). To examine the role of P*asqseC*, a deletion beginning downstream of *qseC* and extending through to the end of *qseC2* (ΔP*asqseC*Δ*qseC2*), was constructed in R7A and R7A* (Figure 4A). In the R7A background this deletion stimulated excision and conjugative transfer to levels similar to those of R7A* (R7AΔP*asqseC*Δ*qseC2* and R7A*ΔP*asqseC*Δ*qseC2*, Figure 2 and Supplementary Table S3). This result suggested P*asqseC* was indeed responsible for preventing R7A cells from entering the R7A* state, possibly through RNA-mediated repression or interference with *qseC* transcription or translation.

To test if anti-*qseC* RNA was able to repress the R7A* phenotype *in trans*, we cloned a region spanning from the likely P*asqseC* transcriptional start site (Figure 4A) through to the start codon of *qseC*, downstream of the strong *nptII* promoter in pPR3G. Introduction of this plasmid into the P*asqseC*-deletion strains described above did not repress AHL production (data not shown), suggesting that the mechanism of antisense regulation might only function *in cis* (41). To test this, we constructed mutagenesis vectors to replace P*asqseC-qseC2* in the R7A/R7A* chromosome with the *nptII* promoter. Two mutagenesis vectors were constructed, one in which P*nptII* was orientated to drive expression anti-sense to *qseC* analogous to P*asqseC* and another to drive expression away from *qseC*. Each mutagenesis plasmid was used to replace the P*asqseC-qseC2* region in both R7A and R7A*. R7A* carrying the anti-*qseC nptII* promoter ceased producing AHLs, confirming that transcription antisense to *qseC* converted R7A* cells back to an R7A-like state. Conversely, R7A carrying the *nptII* promoter in the forward orientation became activated for AHL production, while there was no change in AHL production observed for R7A* (Supplementary Figure S7).

Introduction of pNqseC2 into the ΔP*asqseC*Δ*qseC2*-deletion mutants had no discernible effect on their already-elevated levels of AHL production or excision (Figure 2). Likewise, no changes in AHL-production phenotypes were observed following introduction of pNqseC2 into any of the constructed strains carrying the *nptII* promoter (Supplementary Figure S7). Taken together, these results suggested P*asqseC* expression determined the R7A* AHL-production phenotype and that QseC2 controlled P*asqseC* expression. We further hypothesized that elevated levels of QseC2 in R7A* cells were responsible for the repression of P*asqseC* and derepression of *qseC* transcription and/or translation and that this in turn led to the QseC-mediated repression of *qseM*, the activation of TraR and FseA and, ultimately, TraR-mediated activation of QS and FseA-mediated activation of ICE*Ml*Sym^{R7A} excision.

QseC2 binds two operator sites and represses P*asqseC* and P*qseC2*

qseC2 is located downstream of a pair of inverted repeat sequences $O2_L$ and $O2_R$ that seemed likely QseC2 binding sites. We purified hexahistidine-tagged QseC2 (6H-QseC2) and used this in EMSAs with a 106-bp DNA region spanning from the predicted transcriptional start site of P*asqseC* through to the start of the *qseC2* gene, containing the putative QseC2 operators $O2_L$ and $O2_R$ (Figure 4B). DNA containing wild-type operators exhibited two distinct mobility shifts in EMSAs with increasing concentrations of 6H-QseC2, consistent with 6H-QseC2 binding one site and then a second site in a concentration-dependent manner. EMSAs performed using DNA with scrambled $O2_L$ or $O2_R$ sequences only exhibited single mobility shifts and DNA containing completely scrambled sequence was not shifted. QseC2 shifted DNA containing individual $O2_L$ or $O2_R$ operators with similar affinity, but with a slight preference for $O2_L$. QseC2 exhibited comparatively weaker affinity for its operator sites than QseC does with O_L and O_R (15). In previous work, a 17-fold excess of 6H-QseC (monomeric) shifted both O_L and O_R (15), whereas here a 64-fold molar excess of 6H-QseC2 was needed to observe a full shift of both $O2_L$ and $O2_R$. There was also less evidence for QseC2 cooperativity in the binding of $O2_L$ and $O2_R$ than for QseC with its binding sites. In our previous EMSAs (15), 6H-QseC was unable to fully shift the O_R site when present in isolation even when present in ∼220-fold molar excess, whereas 6H-QseC2 here fully shifted $O2_L$ and $O2_R$ at comparable concentrations.

Surface plasmon resonance (SPR)-based DNA-binding assays (42) were also used to compare binding of each protein with each of the identified operator sites (Figure 4C and Supplementary Table S5). At concentrations of 1 μM, 6H-QseC2 induced a SPR response 183–210% of the the-

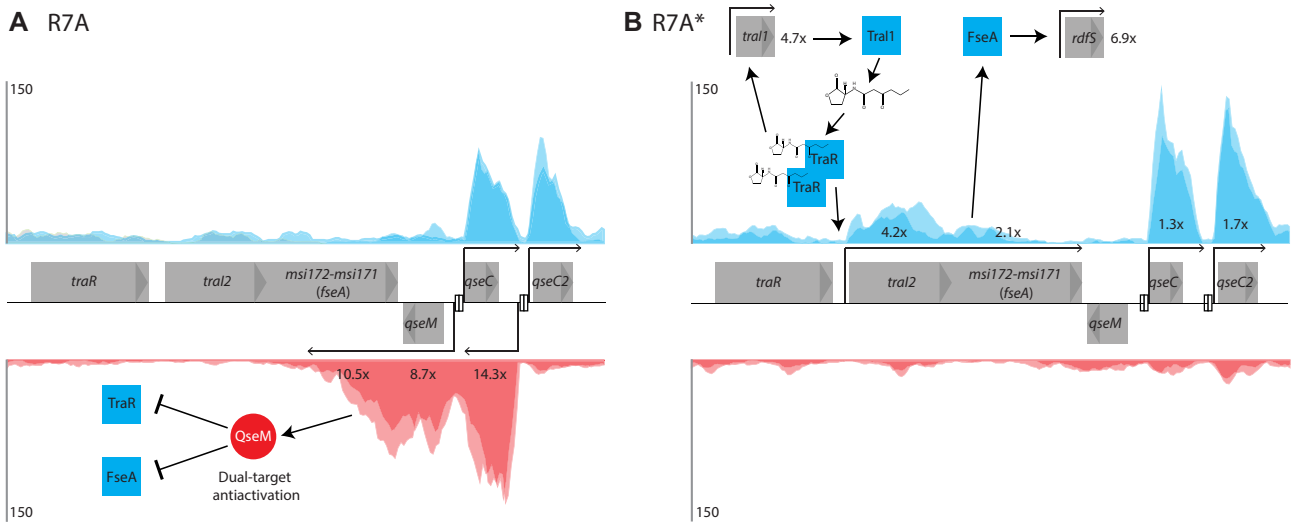

Figure 3. Transcriptome sequencing of R7A and R7A* in the *traR-qseC2* region. Gene maps of the *traR-qseC2* region are shown between coverage maps (*y*-axis represents moving 20-bp average of reads per nucleotide) for strand-specific RNA-seq reads from (**A**) R7A and (**B**) R7A* cells, together with a schematic highlighting proteins involved in activation (blue) and repression (red) of quorum sensing and ICE*Ml*Sym^{R7A} excision and transfer. Genes are indicated as gray blocks and RNA-seq read-depth averages from two experiments are shaded on the *y*-axis in blue for the forward strand and orange for the reverse strand. Positions of QseC and QseC2 operator sites are indicated as vertical rectangles. Numbers underneath genes in (A) represent average mRNA abundance fold-change relative to R7A* and numbers above genes in (B) represent abundance fold-change relative to R7A.

oretical maximum (R_{max}) expected for binding of a single DNA site, as would be expected for 6H-QseC2 dimers simultaneously binding both $O2_L$ and $O2_R$. 6H-QseC2 exhibited a slightly stronger response for the left operator sequence $O2_L$ (115%) than to $O2_R$ (80–86%) (Figure 4C). Purified 6H-QseC produced 165% of R_{max} when assayed with wild-type O_L and O_R together. Consistent with our previous work, 6H-QseC produced a much stronger response to O_L (106% R_{max}) than to O_R (34% R_{max}) (Figure 4C). Using a lower concentration of 0.1 μM, 6H-QseC produced 85% R_{max} for O_L and O_R, 91% for O_L alone, but only 13% for O_R alone. In contrast, 6H-QseC2 produced <14% R_{max} for any of the oligonucleotides tested when used at the lower 0.1 μM concentration, consistent with 6H-QseC2 exhibiting a weaker binding affinity for its operator sites. Neither 6H-QseC nor 6H-QseC2 induced a SPR response with the other protein's cognate operator sequences, confirming regulatory independence of QseC2 and QseC with respect to DNA binding. In summary, like QseC, QseC2 binds two adjacent operator sequences between divergent overlapping promoters; however, in contrast with QseC, QseC2 exhibits overall weaker affinity for its operator sites and only weakly favors the $O2_L$ site.

To test if QseC2 regulated P*asqseC* and/or P*qseC2*, we used the pSDz vector, which carries two cloning cassettes. One cassette is adjacent to a promoterless *lacZ* gene, while a second physically separated and divergently orientated cassette is positioned downstream of an IPTG-inducible *lac* promoter, which itself is located downstream of a *lacI*^{q} gene (Figure 4D) (18). We previously noted that the *lac* promoter on pSDz is expressed at a low level in TY medium in the absence of IPTG, and expression is further induced with IPTG (35). We exploited this inducibility to examine how varying *qseC2* expression levels might impact expression from P*asqseC* and P*qseC2* through concentration-dependent occupancy of $O2_L$ and $O2_R$. A fragment containing P*asqseC* and P*qseC2* was cloned in both orientations upstream of the *lacZ* gene in pSDz. Constructs additionally carrying the *qseC2* gene downstream of the *lac* promoter were derived from the two reporter plasmids and all plasmids were introduced in R7ANS to avoid interference from ICE*Ml*Sym^{R7A}-derived QseC2. β-Galactosidase assays performed using the P*qseC2* promoter construct (Figure 4E(i)) revealed that, unlike P*qseC* which requires activation by QseC (15), P*qseC2* was strongly expressed in the absence of *qseC2*. Assays with P*qseC2* additionally carrying *qseC2* revealed P*qseC2* expression was slightly reduced by uninduced/leaky *qseC2* expression but was repressed ∼9-fold in the presence of IPTG-induced *qseC2* expression. Assays of the P*asqseC* reporter fusion (Figure 4E(ii)) revealed it was expressed at a similar level to P*qseC2* in the absence of *qseC2*, but was repressed to the level of the empty pSDz control with either uninduced or IPTG-induced *qseC2* expression. Thus, while a low level of QseC2 was sufficient to repress P*asqseC* expression, IPTG induction of *qseC2* and thus a higher level of QseC2 was required to repress transcription from P*qseC2*. These observations are consistent with a model in which QseC2 is a transcriptional repressor of P*asqseC* through binding $O2_L$ but only represses its own expression from P*qseC2* when higher concentrations of QseC2 enable occupancy of both $O2_L$ and $O2_R$.

Transient overexpression of QseC2 triggers epigenetic maintenance of the R7A* state

Since the R7A* state appears to be epigenetically maintained, QseC2 and/or QseC concentrations must remain at an elevated level once the R7A* state is established. To test this hypothesis directly, pNqseC2 was modified to carry the *sacB* gene to enable curing from cells by grow-

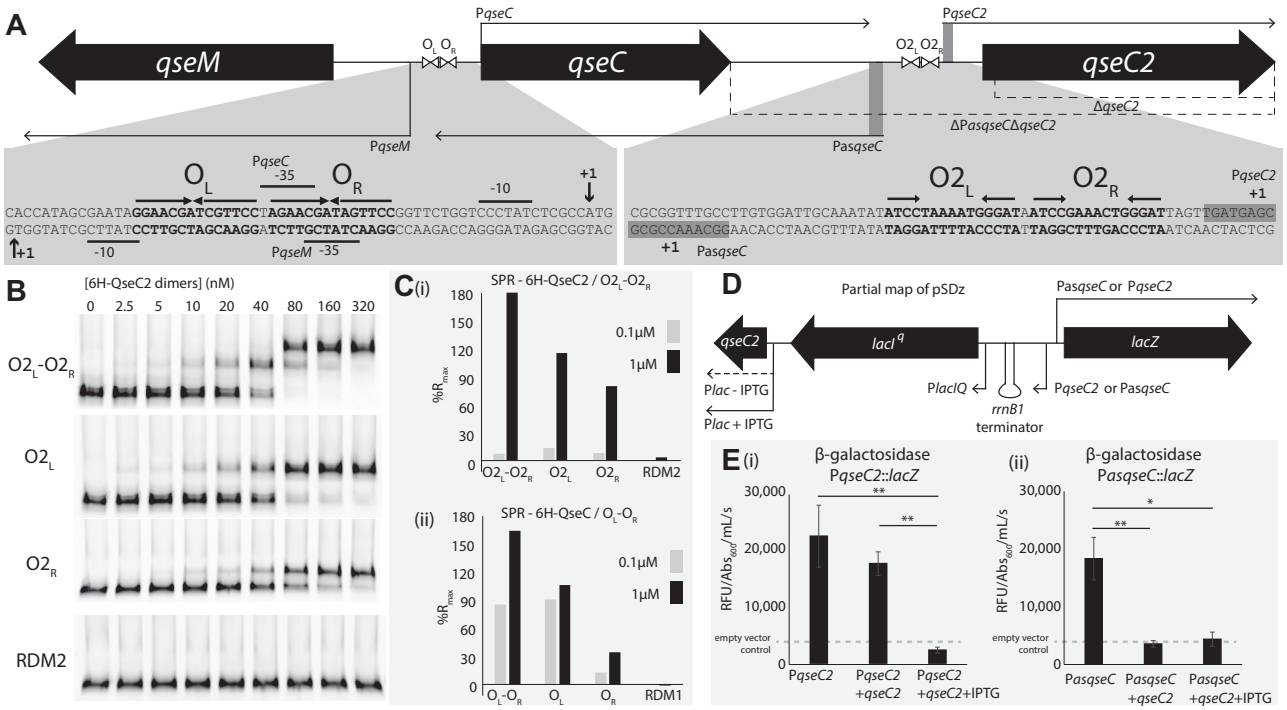

Figure 4. QseC2 binds $O2_L$ and $O2_R$ and represses transcription from P*qseC2* and P*asqseC*. (**A**) A gene map of the *qseM-qseC2* region (to scale). DNA operator sequences are shown below the map. The promoters P*qseM* and P*qseC* were mapped previously (15). Approximate transcription start positions for *asqseC* and *qseC2* were manually estimated from transcriptome alignments (gray highlight). The positions of the constructed Δ*qseC2* and ΔP*asqseC*Δ*qseC2* deletions are indicated with dashed lines. (**B**) Electrophoretic Mobility Shift Assays (EMSAs) using purified 6H-QseC2 with fluorescently labeled dsDNA oligonucleotides containing the $O2_L$-$O2_R$ sequence. The top EMSA labeled $O2_L$-$O2_R$ was carried out using dsDNA containing the wild-type $O2_L$-$O2_R$ sequence; the $O2_L$ EMSA used DNA carrying a scrambled $O2_R$ sequence; the $O2_R$ EMSA used DNA carrying a scrambled $O2_L$ sequence and both operators were scrambled in DNA for the RDM2 EMSA. All assays were carried out using a final concentration of 5 nM labeled dsDNA. (**C**) SPR responses for purified 6H-QseC2 (i) and 6H-QseC (ii) with their cognate operator sequences and mutated derivatives as described in (B). R_{max} is the theoretical maximum binding response assuming 6H-QseC and 6H-QseC2 each bind as dimers to an individual operator (i.e. dimers bound to both operators would have a theoretical R_{max} of 200%). Proteins were added at either 0.1 or 1 μM concentration as indicated. (**D**) Partial gene map (not to scale) of pSDz containing cloned P*asqseC* or P*qseC2* upstream of *lacZ*, and *qseC2* (when present) under control of P*lac*, which exhibits leaky expression in the absence of IPTG (dashed arrow) or elevated expression in the presence of IPTG. (**E**) β-Galactosidase activity of stationary-phase R7ANS cultures containing pSDz plasmid constructs with P*qseC2* (i) or P*asqseC* (ii) oriented to drive transcription of the *lacZ* gene. Modified versions of these constructs harboring *qseC2* under control of the *lac* promoter were also assayed, with or without 1 mM IPTG as indicated. β-Galactosidase activity was measured using the fluorescent substrate 4-methylumbelliferyl-β-D-galactopyranoside (40). Bars represent the mean of four biological replicates and error bars represent standard error of the mean. Statistical significance values from Student's t-test are represented by asterisks (< 0.05 * or < 0.01 **). The mean expression and standard error values for pSDz lacking any cloned promoter (indicated approximately by a dashed line in both (i) and (ii)) were 3,374 ± 127 and 3,542 ± 1,128 with IPTG.

ing on sucrose medium (S/RDM). pNqseC2-sacB and the control plasmid pPR3G-sacB were each introduced into R7A via conjugation in five separate mating experiments. As expected, AHL production was activated in each of the R7A strains carrying pNqseC2-sacB but not in strains carrying plasmid pPR3G-sacB (Supplementary Figure S8A). Stationary-phase broth cultures were inoculated from the five R7A/pNqseC2-sacB strains and grown without selection. Dilutions were spread on sucrose medium to select for loss of pNqseC2-sacB or pPR3G-sacB. Individual colonies isolated from these plates were further single-colony-purified on S/RDM and once more on G/RDM. Each strain was also checked for lack of growth on Gm-containing medium to confirm loss of the plasmids. Passaged single colonies from the G/RDM plates were then used to inoculate TY broths. CV026 bioassays of the supernatants of these broths revealed that each of the strains previously carrying pNqseC2-sacB remained activated for AHL production (Supplementary Figure S8A) and QPCR confirmed these strains exhibited excision frequencies indistinguishable from R7A* (Supplementary Figure S8B). In summary, through introduction of pNqseC2-sacB, R7A cells were artificially induced to enter the R7A* state by *qseC2* overexpression from a plasmid and they remained in this state following curing of this plasmid.

Both QseC and QseC2 are required for maintenance of the R7A* state

Since the transient introduction of pNqseC2-sacB stimulated cells to enter the R7A* state, this suggested chromosomally-encoded QseC and/or QseC2 maintained the R7A* state through autoregulation following the curing of pNqseC2-sacB. To confirm if QseC2 was required for R7A* maintenance, we introduced pNqseC2-sacB into R7AΔ*qseC2* (in 5 separate mating experiments) and then cured the plasmid as described above. pNqseC2-sacB induced AHL production in R7AΔ*qseC2* as expected; how-

ever, R7AΔ*qseC2* ceased producing AHLs following curing of pNqseC2-sacB, confirming that the chromosomal *qseC2* gene was essential for R7A* maintenance (Supplementary Figure S8A).

It remained unclear if the QseC protein was critically involved in maintaining the R7A* state as it seemed possible QseC2 alone might stimulate and maintain the phenotypes by directly repressing read-through transcription of *qseM* from the P*asqseC* promoter. To abolish translation of QseC without disrupting surrounding regulatory elements, we introduced an amber mutation into the *qseC* gene. A 3-bp change was introduced to convert the 10th codon to TAG; this change also removed a downstream ATG codon and introduced an overlapping XbaI restriction-endonuclease site for mutant screening. This mutation was constructed in R7A and R7A*, producing strains R7A*qseC*(Am) and R7A**qseC*(Am). AHL production was abolished in R7A**qseC*(Am). Introduction of pNqseC2-sacB did not induce AHL production in R7A*qseC*(Am) or R7A**qseC*(Am) (Supplementary Figure S9). Translation of *qseC* was therefore essential for both R7A* establishment and maintenance. In summary, QseC and QseC2 together, coupled through anti-*qseC* transcription from P*asqseC*, form the epigenetic switch controlling entry into the transfer-primed R7A* state.

DISCUSSION

In this work we showed that a subpopulation of R7A cells can transition into a stable state we termed R7A*, which exhibits upregulated AHL production, ICE*Ml*Sym^{R7A} excision and horizontal transfer. RNA sequencing of R7A* cells revealed they were nearly abolished for *qseM* mRNA, explaining the derepression of phenotypes normally inhibited through QseM interactions with TraR and FseA. The R7A* state appeared spontaneously in cells within ∼2% of colonies derived from stationary-phase cultures. Extensive genome sequencing failed to identify structural or genetic changes that could likely explain the R7A* phenotypes. R7A* cells heritably maintained their phenotypes under standard laboratory culture conditions. The R7A* state was not transferred along with ICE*Ml*Sym^{R7A} from R7A* to the non-symbiotic isogenic recipient R7ANS*, indicating that inheritance of the R7A* state depended on factors present in the donor cell that were not transferred with DNA to the recipient during conjugation and that the R7A* state did not involve a heritable factor associated with the R7A* chromosome. In summary, R7A* cells are epigenetically maintained in a state primed for QS and horizontal transfer.

In previous work we proposed that a molecular switch comprising QseC and its operator sequences facilitated bimodal repression of *qseM* and that individual cells in R7A populations were either in an 'on-state' or 'off-state' for QS, ICE*Ml*Sym^{R7A} excision and conjugative transfer (Figure 1) (15). This was based on the findings that the -35 regions of P*qseC* and P*qseM* are located within O_R, *qseM* RNA is more abundant in a *qseC* mutant and expression from P*qseC* is activated by QseC (15). Therefore, in conditions where QseC is absent or at low concentration, e.g. following entry of ICE*Ml*Sym^{R7A} into a new host, expression of

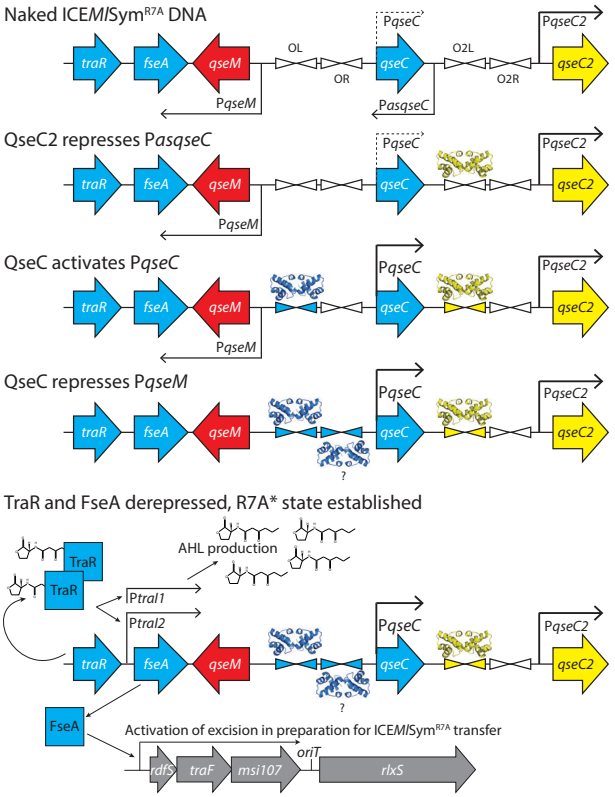

Figure 5. Model of the molecular steps leading to the R7A* state. Abridged gene maps (not to scale) illustrate regulatory steps involved in transition into the R7A* state. In the absence of any of the protein regulators (for example in a recipient upon receiving ICE*Ml*Sym^{R7A} immediately post-transfer), P*qseM*, P*asqseC* and P*qseC2* promoters are active. Once QseC2 concentrations increase above a certain threshold, QseC2 binds $O2_L$ and represses P*asqseC*. Repression of P*asqseC* derepresses the translation of QseC through an unknown antisense mechanism. QseC activates expression from its own promoter through binding O_L. QseC also represses P*qseM* and, based on the position of the P*qseM* -35 region, this repression may involve QseC-dimer occupancy of both O_L and O_R (indicated by a question mark) (15). Once QseM concentrations decrease, TraR is free to activate QS through activation of the P*traI1*. TraR activation of P*traI2* leads to expression of FseA, which in turn leads to expression of P*rdfS*.

qseC is weak while *qseM* expression is strong, thus keeping cells repressed for QS and excision. Once QseC concentrations reach some critical threshold, QseC binds to O_L, further activating its own expression. QseC also represses the P*qseM* promoter, either by binding O_L alone, or as previously speculated through cooperative binding of O_L and O_R (Figure 5). This results in the derepression of TraR and FseA and the subsequent activation of QS and horizontal transfer. In this work we discovered that QseC-dependent repression of P*qseM* is itself inhibited by transcription from the P*asqseC* promoter, which produces RNA antisense to *qseC*. Deletion of the P*asqseC* promoter stimulated cells to enter an R7A*-like state. We also discovered that a second adjacently encoded C-protein, QseC2, bound a distinct set of operator sites and repressed transcription from P*asqseC*. Overexpression of QseC2 also stimulated cells to enter an R7A*-like state. In summary, QseC2 represses P*asqseC*, which likely enables QseC concentrations to increase and

repress P*qseM*. The resultant absence of QseM allows TraR to activate FseA, which in turn activates P*rdfS* (Figure 5).

Introduction of a stop codon into *qseC* prevented establishment of the R7A* state, confirming the R7A* state depends on active QseC protein. Deletion of the *qseC*-antisense promoter P*asqseC* caused R7A cells to enter an R7A*-like state, suggesting P*asqseC* somehow reduces QseC levels and prevents QseC-mediated repression of P*qseM*. Several mechanisms of antisense-RNA regulation have been characterized in prokaryotes (41). One possibility for regulation by P*asqseC* is that transcription from this promoter results in antisense RNA that anneals with *qseC* transcripts and the resultant dsRNA is targeted for RNase degradation. However, plasmid-based overexpression of antisense-*qseC* RNA from the *nptII* promoter did not complement a strain carrying a P*asqseC* deletion. This could suggest transcription from P*asqseC* is only effective in repressing QseC levels when it occurs *in cis* with *qseC* (43). Supporting this hypothesis, replacement of P*asqseC* with the *nptII* promoter to drive antisense-*qseC* transcription switched off AHL production in R7A*. The P*asqseC* promoter could cause a reduction in *qseC* mRNA through *cis*-acting transcriptional interference, whereby RNA polymerases on opposite DNA strands occlude or terminate each other's transcription initiation or elongation (44). However, the RNA-seq data did not indicate any reduction in *qseC* mRNA abundance to support either a dsRNA degradation or a *cis*-acting transcriptional interference mechanism. The abundance of full-length *qseC* mRNA in R7A cells was not significantly different from that observed in R7A* and there was no obvious evidence for degradation of *qseC* transcripts in R7A compared to R7A* (Figure 3B). In prokaryotes, translation inhibition via antisense RNA can occur through antisense binding to the sense mRNA in such a way that the Shine-Dalgarno sequence is occluded from the ribosome. Again, this mechanism seems unlikely since *qseC* mRNA is a leaderless transcript lacking a canonical ribosome-binding site. As far as we are aware, antisense regulation of leaderless mRNA transcripts remains an unexamined phenomenon. While we were unable to resolve the exact mechanism of P*asqseC*-mediated repression of QseC, the observations nevertheless provide the first insights into how tandemly-coded C-protein genes can be genetically combined to form higher-order switches. Tandemly-coded C-protein genes with distinct operator sequences are present on other ICEs (15,22,32), suggesting that the genetic and molecular coupling of tandemly coded pairs of C-protein genes could be a common evolutionary solution for the assembly of highly stable genetic switches.

Overexpression of *qseC2* from plasmid pNqseC2-sacB induced R7A cells to enter the R7A* state and cells remained in the R7A* state even after curing of pNqseC2-sacB. The phenotypes were not maintained in strains carrying mutations in either *qseC* or *qseC2*, confirming both proteins are required to epigenetically maintain the R7A* state. This implies that once the state is established, concentrations of QseC and QseC2 proteins remain elevated compared to those in R7A cells. For QseC2, the ∼1.7-fold increase in *qseC2* mRNA in R7A* compared to R7A may be enough to account for this (Figure 3). As demonstrated in our promoter fusion assays using IPTG-inducible *qseC2*, even leaky uninduced expression of *qseC2* from the *lac* promoter strongly repressed transcription from P*asqseC*. QseC2 only strongly repressed its own promoter following IPTG induction. The elevated levels of *qseC2* mRNA in R7A* suggest in most R7A* cells QseC2 levels are not high enough to trigger such negative autoregulation or, more likely, any negative autoregulation by QseC2 is short-lived due to the resulting decline in QseC2 concentration and derepression of P*qseC2*. The negative autoregulation observed for QseC2 likely serves to maintain a moderately-elevated equilibrium concentration of QseC2 in R7A* that is high enough to strongly repress P*asqseC* but not P*qseC2*. While the levels of *qseC* sense mRNA were not significantly different in R7A* compared to R7A, antisense-*qseC* RNA was almost completely absent from R7A. As discussed above, repression of P*asqseC* derepresses QseC-mediated repression of P*qseM*, strongly suggesting P*asqseC* represses QseC translation or activity either directly or indirectly. It remains unclear what triggers the initial increases in QseC2 and/or QseC during entry into the R7A* state but it is plausible this is a stochastic process resulting from uneven initial concentrations of QseC and/or QseC2 following cell division. Future experiments examining the cellular concentrations of QseC and QseC2 in R7A and R7A* may resolve these questions.

While not interrogated here, our RNA-seq experiments also revealed a global downregulation of ribosomal protein genes in R7A* with a 4- to 14-fold reduction in mRNA abundance for 46 ribosomal-subunit genes (Dataset S2). Downregulation of ribosome synthesis is commonly observed in cells experiencing nutritional deficiencies or other forms of stress. In diverse bacteria repression of ribosome synthesis can be stimulated by an increase in concentration of the alarmone molecule ppGpp, a phenomenon termed the stringent response. ppGpp together with the DksA protein binds RNA polymerase and decreases transcription from rRNA promoters, while activating pathways in amino-acid biosynthesis (45,46). The transcriptome of R7A* was not entirely consistent with the stringent response as several of the most upregulated genes were involved in arginine catabolism (including 8-fold increases in arginase and ornithine deaminase genes, R7A2020_27410 and R7A2020_27415, Dataset S2). Regardless, changes in ribosomal protein abundance might provide a mechanism to trigger and/or maintain the R7A* state. Various stress conditions can alter ribosome composition and selectively enhance translation of leaderless mRNAs (47,48). Increased leaderless mRNA translation is at least partly stimulated through downregulation of the redox-regulated ATPase YchF, which normally represses translation from leaderless mRNA through interactions with translation initiation-factor-3 (48). A 3.5-fold reduction in mRNA abundance was observed for the *ychF* gene in R7A* (R7A2020_10900, Dataset S2), suggesting translation from leaderless mRNAs like *qseC* (and possibly *qseC2*) may be enhanced in R7A* cells.

The observation that R7A* exhibits slightly lower excision frequencies and a ∼2- to 3-fold lower conjugation frequency than R7AΔ*qseM* could indicate the presence of a subpopulation of cells in the R7A* population that have reverted to a QS and transfer 'off' state like most R7A cells. Several attempts were made to isolate cells from R7A*

populations that had reverted to a state resembling R7A; however, it appears that the reversion rate is at least lower than the R7A > R7A* conversion rate (Supporting Information). In our attempts to isolate R7A* revertants, we isolated several colonies that had seemingly lost the ability to make AHL, but they all regained the ability to make AHL following further subculture. We suspect these R7A-like cells derived from R7A* had likely inherited lower QseC2/QseC protein concentrations than most R7A* cells and therefore exhibited higher expression of *qseM* (repressing QS) but that the levels of QseC2/QseC were still above the concentration required to re-establish the R7A* state through repression of P*qsqseC* and positive autoregulation of *qseC* expression. We only observed a complete reset of the R7A* switch state in recipients of ICE*Ml*Sym^{R7A} following conjugative transfer. By analogy with RM systems, conversion to the R7A* state resembles the delayed activation of restriction endonuclease expression following entry of an RM system into a naïve cell, where neither the C protein nor the endonuclease are expressed highly until such time as C-protein concentrations increase above a certain threshold. However, once the RM system becomes established in the cell, C-protein concentrations do not revert back to a naïve state until the RM system is transferred to a naïve host. Like establishment of an RM system, it seems possible that induction of the R7A* state in donor populations may be an epigenetically permanent switch.

The generation of two distinct phenotypic states within a genetically identical population, often termed bistability, effectively enables bacterial populations to 'hedge their bets' (49) on future natural selection events. Phenotypes regulated by bistability include induction of bacterial sporulation (50), DNA competence (51), antimicrobial-resistant persister cell formation (52), motility (53) and transfer of other ICEs (54). We and others have proposed bistable regulation of ICE transfer (and likely transfer of other mobile elements) allows ICEs to benefit from stable vertical descent with minimal impact to their current host organism, whilst simultaneously partitioning a small proportion of cells from each generation to become primed for ICE transfer and bear any associated impacts on host fitness (15,54,55). Regulation of transfer of ICE*clc* from *Pseudomonas knackmussii* B13 seems to illustrate this model well. ICE*clc*, induces a proportion of the *P. knackmussii* B13 population to differentiate into cells derepressed for transfer functions (56,57). These so-called 'transfer-competent' cells exhibit severely reduced growth and frequent lysis, highlighting the host fitness costs associated with ICE transfer. While our RNA-seq experiments here revealed a global downregulation of ribosomal protein genes and suggested some disruptions to metabolism (Dataset S2), R7A* did not exhibit any obvious fitness disadvantage (Supplementary Figure S1) or display any overt phenotypes suggestive of cells suffering stress. However, the observation that introduction of pJR-traR into R7A* inhibited cell growth in an FseA-dependent manner suggests there may indeed be host fitness impacts of ICE*Ml*Sym^{R7A} transfer but that the stoichiometry of TraR and FseA in transfer-primed R7A* cells is balanced finely enough to avoid these impacts under the conditions tested. It is possible that while R7A* cells are primed for transfer, negative impacts on host fitness may only surface once horizontal transfer has commenced. From this perspective, the study of R7A and R7A* cells represents a unique platform from which to precisely examine potential fitness costs associated with horizontal transfer in isogenic cell populations and expose the intricate molecular mechanisms by which mobile genetic elements mitigate their impact on the host.

DATA AVAILABILITY

All genome assemblies and sequencing read files are available from NCBI BioProject accession PRJNA627051. RNA-seq data are also available through the Gene Expression Omnibus (GEO) series accession GSE189468. Comparisons of R7A and R7A* genome assemblies are presented in Dataset S1 and complete RNA-seq data are presented in Dataset S2.

SUPPLEMENTARY DATA

Supplementary Data are available at NAR Online.

FUNDING

Royal Society of New Zealand Marsden Fund [16-UOO-207 to C.W.R., J.P.R., C.S.B.]; Australian Research Council [FT170100235 to J.P.R]; Natural Sciences and Engineering Research Council (NSERC) (to M.F.H., C.K.Y.). Funding for open access charge: Australian Research Council [FT170100235].
Conflict of interest statement. None declared.

REFERENCES

1. Brockhurst,M.A., Harrison,E., Hall,J.P.J., Richards,T., McNally,A. and MacLean,C. (2019) The ecology and evolution of pangenomes. *Curr. Biol.*, **29**, R1094–R1103.
2. Guglielmini,J., Quintais,L., Garcillan-Barcia,M.P., de la Cruz,F. and Rocha,E.P. (2011) The repertoire of ICE in prokaryotes underscores the unity, diversity, and ubiquity of conjugation. *PLoS Genet.*, **7**, e1002222.
3. Hall,J.P.J., Brockhurst,M.A., Dytham,C. and Harrison,E. (2017) The evolution of plasmid stability: Are infectious transmission and compensatory evolution competing evolutionary trajectories? *Plasmid*, **91**, 90–95.
4. Hall,J.P., Wood,A.J., Harrison,E. and Brockhurst,M.A. (2016) Source-sink plasmid transfer dynamics maintain gene mobility in soil bacterial communities. *Proc. Natl. Acad. Sci. U.S.A.*, **113**, 8260–8265.
5. Danino,V.E., Wilkinson,A., Edwards,A. and Downie,J.A. (2003) Recipient-induced transfer of the symbiotic plasmid pRL1JI in *Rhizobium leguminosarum* bv. *viciae* is regulated by a quorum-sensing relay. *Mol. Microbiol.*, **50**, 511–525.
6. Oger,P. and Farrand,S.K. (2002) Two opines control conjugal transfer of an *Agrobacterium* plasmid by regulating expression of separate copies of the quorum-sensing activator gene *traR*. *J. Bacteriol.*, **184**, 1121–1131.
7. Poulin-Laprade,D. and Burrus,V. (2015) A lambda Cro-like repressor is essential for the induction of conjugative transfer of SXT/R391 elements in response to DNA damage. *J. Bacteriol.*, **197**, 3822–3833.
8. Dunny,G.M. and Berntsson,R.P. (2016) Enterococcal sex pheromones: evolutionary pathways to complex, two-signal systems. *J. Bacteriol.*, **198**, 1556–1562.
9. Martinez-Hidalgo,P., Ramirez-Bahena,M.H., Flores-Felix,J.D., Igual,J.M., Sanjuan,J., Leon-Barrios,M., Peix,A. and Velazquez,E. (2016) Reclassification of strains MAFF 303099^{T} and R7A into *Mesorhizobium japonicum* sp. nov. *Int. J. Syst. Evol. Microbiol.*, **66**, 4936–4941.

10. Remigi,P., Zhu,J., Young,J.P.W. and Masson-Boivin,C. (2016) Symbiosis within symbiosis: evolving nitrogen-fixing legume symbionts. *Trends Microbiol.*, **24**, 63–75.
11. Sullivan,J.T., Trzebiatowski,J.R., Cruickshank,R.W., Gouzy,J., Brown,S.D., Elliot,R.M., Fleetwood,D.J., McCallum,N.G., Rossbach,U., Stuart,G.S. *et al.* (2002) Comparative sequence analysis of the symbiosis island of *Mesorhizobium loti* strain R7A. *J. Bacteriol.*, **184**, 3086–3095.
12. Haskett,T.L., Terpolilli,J.J., Bekuma,A., O'Hara,G.W., Sullivan,J.T., Wang,P., Ronson,C.W. and Ramsay,J.P. (2016) Assembly and transfer of tripartite integrative and conjugative genetic elements. *Proc. Natl. Acad. Sci. U.S.A.*, **113**, 12268–12273.
13. Hill,Y., Colombi,E., Bonello,E., Haskett,T., Ramsay,J., O'Hara,G. and Terpolilli,J. (2020) Evolution of diverse effective N2-fixing microsymbionts of Cicer arietinum following horizontal transfer of the *Mesorhizobium ciceri* CC1192 symbiosis integrative and conjugative element. *Appl. Environ. Microbiol.*, **87**, e02558-20.
14. Sullivan,J.T. and Ronson,C.W. (1998) Evolution of rhizobia by acquisition of a 500-kb symbiosis island that integrates into a *phe*-tRNA gene. *Proc. Natl. Acad. Sci. U. S. A.*, **95**, 5145–5149.
15. Ramsay,J.P., Major,A.S., Komarovsky,V.M., Sullivan,J.T., Dy,R.L., Hynes,M.F., Salmond,G.P. and Ronson,C.W. (2013) A widely conserved molecular switch controls quorum sensing and symbiosis island transfer in *Mesorhizobium loti* through expression of a novel antiactivator. *Mol. Microbiol.*, **87**, 1–13.
16. Ramsay,J.P., Sullivan,J.T., Jambari,N., Ortori,C.A., Heeb,S., Williams,P., Barrett,D.A., Lamont,I.L. and Ronson,C.W. (2009) A LuxRI-family regulatory system controls excision and transfer of the *Mesorhizobium loti* strain R7A symbiosis island by activating expression of two conserved hypothetical genes. *Mol. Microbiol.*, **73**, 1141–1155.
17. Ramsay,J.P., Sullivan,J.T., Stuart,G.S., Lamont,I.L. and Ronson,C.W. (2006) Excision and transfer of the *Mesorhizobium loti* R7A symbiosis island requires an integrase IntS, a novel recombination directionality factor RdfS, and a putative relaxase RlxS. *Mol. Microbiol.*, **62**, 723–734.
18. Ramsay,J.P., Tester,L.G., Major,A.S., Sullivan,J.T., Edgar,C.D., Kleffmann,T., Patterson-House,J.R., Hall,D.A., Tate,W.P., Hynes,M.F. *et al.* (2015) Ribosomal frameshifting and dual-target antiactivation restrict quorum-sensing-activated transfer of a mobile genetic element. *Proc. Natl. Acad. Sci. U.S.A.*, **112**, 4104–4109.
19. Sullivan,J.T., Patrick,H.N., Lowther,W.L., Scott,D.B. and Ronson,C.W. (1995) Nodulating strains of *Rhizobium loti* arise through chromosomal symbiotic gene transfer in the environment. *Proc. Natl. Acad. Sci. U.S.A.*, **92**, 8985–8989.
20. Verdonk,C.J., Sullivan,J.T., Williman,K.M., Nicholson,L., Bastholm,T.R., Hynes,M.F., Ronson,C.W., Bond,C.S. and Ramsay,J.P. (2019) Delineation of the integrase-attachment and origin-of-transfer regions of the symbiosis island ICE*Ml*Sym^{R7A}. *Plasmid*, **104**, 102416.
21. Burrus,V. (2017) Mechanisms of stabilization of integrative and conjugative elements. *Curr. Opin. Microbiol.*, **38**, 44–50.
22. Sorokin,V., Severinov,K. and Gelfand,M.S. (2009) Systematic prediction of control proteins and their DNA binding sites. *Nucleic Acids Res.*, **37**, 441–451.
23. Williams,K., Savageau,M.A. and Blumenthal,R.M. (2013) A bistable hysteretic switch in an activator-repressor regulated restriction-modification system. *Nucleic Acids Res.*, **41**, 6045–6057.
24. McGeehan,J.E., Papapanagiotou,I., Streeter,S.D. and Kneale,G.G. (2006) Cooperative binding of the C.AhdI controller protein to the C/R promoter and its role in endonuclease gene expression. *J. Mol. Biol.*, **358**, 523–531.
25. Bogdanova,E., Djordjevic,M., Papapanagiotou,I., Heyduk,T., Kneale,G. and Severinov,K. (2008) Transcription regulation of the type II restriction-modification system AhdI. *Nucleic Acids Res.*, **36**, 1429–1442.
26. Knowle,D., Lintner,R.E., Touma,Y.M. and Blumenthal,R.M. (2005) Nature of the promoter activated by C.PvuII, an unusual regulatory protein conserved among restriction-modification systems. *J. Bacteriol.*, **187**, 488–497.
27. Mruk,I., Rajesh,P. and Blumenthal,R.M. (2007) Regulatory circuit based on autogenous activation-repression: roles of C-boxes and spacer sequences in control of the PvuII restriction-modification system. *Nucleic Acids Res.*, **35**, 6935–6952.
28. Lopez-Fuentes,E., Torres-Tejerizo,G., Cervantes,L. and Brom,S. (2014) Genes encoding conserved hypothetical proteins localized in the conjugative transfer region of plasmid pRet42a from *Rhizobium etli* CFN42 participate in modulating transfer and affect conjugation from different donors. *Front. Microbiol.*, **5**, 793.
29. Zheleznaya,L.A., Kainov,D.E., Yunusova,A.K. and Matvienko,N.I. (2003) Regulatory C protein of the EcoRV modification-restriction system. *Biochemistry (Mosc.)*, **68**, 105–110.
30. Semenova,E., Minakhin,L., Bogdanova,E., Nagornykh,M., Vasilov,A., Heyduk,T., Solonin,A., Zakharova,M. and Severinov,K. (2005) Transcription regulation of the EcoRV restriction-modification system. *Nucleic Acids Res.*, **33**, 6942–6951.
31. Sorokin,V., Severinov,K. and Gelfand,M.S. (2010) Large-scale identification and analysis of C-proteins. *Methods Mol. Biol.*, **674**, 269–282.
32. Colombi,E., Perry,B.J., Sullivan,J.T., Bekuma,A.A., Terpolilli,J.J., Ronson,C.W. and Ramsay,J.P. (2021) Comparative analysis of integrative and conjugative mobile genetic elements in the genus *Mesorhizobium*. *Microb. Genom.*, **7**, 000657.
33. Beringer,J.E. (1974) R factor transfer in *Rhizobium leguminosarum*. *J. Gen. Microbiol.*, **84**, 188–198.
34. Ronson,C.W., Nixon,B.T., Albright,L.M. and Ausubel,F.M. (1987) *Rhizobium meliloti ntrA* (*rpoN*) gene is required for diverse metabolic functions. *J. Bacteriol.*, **169**, 2424–2431.
35. Haskett,T.L., Terpolilli,J.J., Ramachandran,V.K., Verdonk,C.J., Poole,P.S., O'Hara,G.W. and Ramsay,J.P. (2018) Sequential induction of three recombination directionality factors directs assembly of tripartite integrative and conjugative elements. *PLoS Genet.*, **14**, e1007292.
36. Kolmogorov,M., Yuan,J., Lin,Y. and Pevzner,P.A. (2019) Assembly of long, error-prone reads using repeat graphs. *Nat. Biotechnol.*, **37**, 540–546.
37. Walker,B.J., Abeel,T., Shea,T., Priest,M., Abouelliel,A., Sakthikumar,S., Cuomo,C.A., Zeng,Q., Wortman,J., Young,S.K. *et al.* (2014) Pilon: an integrated tool for comprehensive microbial variant detection and genome assembly improvement. *PLoS One*, **9**, e112963.
38. Yui Eto,K., Kwong,S.M., LaBreck,P.T., Crow,J.E., Traore,D.A.K., Parahitiyawa,N., Fairhurst,H.M., Merrell,D.S., Firth,N., Bond,C.S. *et al.* (2021) Evolving origin-of-transfer sequences on staphylococcal conjugative and mobilizable plasmids-who's mimicking whom? *Nucleic Acids Res.*, **49**, 5177–5188.
39. Stevenson,C.E., Assaad,A., Chandra,G., Le,T.B., Greive,S.J., Bibb,M.J. and Lawson,D.M. (2013) Investigation of DNA sequence recognition by a streptomycete MarR family transcriptional regulator through surface plasmon resonance and X-ray crystallography. *Nucleic Acids Res.*, **41**, 7009–7022.
40. Ramsay,J.P. (2013) High-throughput β-galactosidase and β-glucuronidase assays using fluorogenic substrates. *Bio-protocol*, **3**, e827.
41. Georg,J. and Hess,W.R. (2018) Widespread antisense transcription in prokaryotes. *Microbiol. Spectr.*, **6**, RWR-0029.
42. Stevenson,C.E.M. and Lawson,D.M. (2021) Analysis of protein-DNA interactions using surface plasmon resonance and a ReDCaT chip. *Methods Mol. Biol.*, **2263**, 369–379.
43. Saberi,F., Kamali,M., Najafi,A., Yazdanparast,A. and Moghaddam,M.M. (2016) Natural antisense RNAs as mRNA regulatory elements in bacteria: a review on function and applications. *Cell Mol. Biol. Lett.*, **21**, s11658-016-0007-z.
44. Andre,G., Even,S., Putzer,H., Burguiere,P., Croux,C., Danchin,A., Martin-Verstraete,I. and Soutourina,O. (2008) S-box and T-box riboswitches and antisense RNA control a sulfur metabolic operon of *Clostridium acetobutylicum*. *Nucleic Acids Res.*, **36**, 5955–5969.
45. Gourse,R.L., Chen,A.Y., Gopalkrishnan,S., Sanchez-Vazquez,P., Myers,A. and Ross,W. (2018) Transcriptional responses to ppGpp and DksA. *Annu. Rev. Microbiol.*, **72**, 163–184.
46. Sanchez-Vazquez,P., Dewey,C.N., Kitten,N., Ross,W. and Gourse,R.L. (2019) Genome-wide effects on *Escherichia coli* transcription from ppGpp binding to its two sites on RNA polymerase. *Proc. Natl. Acad. Sci. U.S.A.*, **116**, 8310–8319.
47. Vesper,O., Amitai,S., Belitsky,M., Byrgazov,K., Kaberdina,A.C., Engelberg-Kulka,H. and Moll,I. (2011) Selective translation of leaderless mRNAs by specialized ribosomes generated by MazF in *Escherichia coli*. *Cell*, **147**, 147–157.

48. Landwehr,V., Milanov,M., Angebauer,L., Hong,J., Jungert,G., Hiersemenzel,A., Siebler,A., Schmit,F., Ozturk,Y., Dannenmaier,S. *et al.* (2021) The universally conserved ATPase YchF regulates translation of leaderless mRNA in response to stress conditions. *Front. Mol. Biosci.*, **8**, 643696.
49. Veening,J.W., Smits,W.K. and Kuipers,O.P. (2008) Bistability, epigenetics, and bet-hedging in bacteria. *Annu. Rev. Microbiol.*, **62**, 193–210.
50. Chung,J.D., Stephanopoulos,G., Ireton,K. and Grossman,A.D. (1994) Gene expression in single cells of *Bacillus subtilis*: evidence that a threshold mechanism controls the initiation of sporulation. *J. Bacteriol.*, **176**, 1977–1984.
51. Maamar,H. and Dubnau,D. (2005) Bistability in the *Bacillus subtilis* K-state (competence) system requires a positive feedback loop. *Mol. Microbiol.*, **56**, 615–624.
52. Balaban,N.Q., Merrin,J., Chait,R., Kowalik,L. and Leibler,S. (2004) Bacterial persistence as a phenotypic switch. *Science*, **305**, 1622–1625.
53. Kearns,D.B. and Losick,R. (2005) Cell population heterogeneity during growth of *Bacillus subtilis*. *Genes Dev.*, **19**, 3083–3094.
54. Minoia,M., Gaillard,M., Reinhard,F., Stojanov,M., Sentchilo,V. and van der Meer,J.R. (2008) Stochasticity and bistability in horizontal transfer control of a genomic island in *Pseudomonas*. *Proc. Natl. Acad. Sci. U.S.A.*, **105**, 20792–20797.
55. Ramsay,J.P. and Ronson,C.W. (2015) Silencing quorum sensing and ICE mobility through antiactivation and ribosomal frameshifting. *Mob. Genet. Elements*, **5**, 103–108.
56. Reinhard,F., Miyazaki,R., Pradervand,N. and van der Meer,J.R. (2013) Cell differentiation to "mating bodies" induced by an integrating and conjugative element in free-living bacteria. *Curr. Biol.*, **23**, 255–259.
57. Pradervand,N., Sulser,S., Delavat,F., Miyazaki,R., Lamas,I. and van der Meer,J.R. (2014) An operon of three transcriptional regulators controls horizontal gene transfer of the integrative and conjugative element ICE*clc* in *Pseudomonas knackmussii* B13. *PLoS Genet.*, **10**, e1004441.